Transactions of the Korean Nuclear Society Virtual Spring Meeting
July 9-10, 2020

Analysis of Errors from Various Origins in Pin-Homogenized Multi-Group Calculation

Hyunsik Hong and Han Gyu Joo*
Department of Nuclear Engineering, Seoul National University,
1 Gwanak-ro, Gwanak-gu, Seoul, 08826 Korea
**Corresponding author: joohan@snu.ac.kr*

1. Introduction

The development of pin-by-pin multi-group (MG) core calculation codes such as SCOPE2 of NFI [1] and DYN3D of HZDR [2] has been carried out by numerous groups. It aims at filling the gap between the conventional two-step calculation (TSC) employing assembly-homogenized few-group constants (few-GCs) and the direct whole core calculation (DWC) being performed with explicit heterogeneous core geometries and tens of energy groups. Although DWCs has the advantage of incorporating the actual core environment accurately to yield high fidelity solutions, it is not practical because it demands significantly higher computing resource than TSCs. On the contrary, pin-by-pin MG calculation (PPMGC) requires manageable computing resources which industry can afford while it yields remarkably improved solutions over the TSC results [3]. In generally, the pin-level finite difference (FD) or nodal calculations to solve the simplified PN (SPN) equation is employed in PPMGCs along with the superhomogenization (SPH) factors [4] or the generalized equivalence theory (GET) [5] parameters which are to take the pin-cell homogenization effect into account.

The SPHINCS code [6] being developed at SNU solves either the diffusion or SP3 equation using the finite difference method (FDM) to save the computing time by taking the advantage of small mesh sizes. The SPH factors are employed to account for the pin-cell homogenization effect and the spatial truncation error of the FDM. For a series of test calculations including the two-dimensional (2-D) initial core of AP1000® and APR1400 PWRs, the SPHINCS solutions agree quite well with the reference transport solutions. Nontrivial errors are, however, observed for highly heterogeneous problems [7]. Although the pin-wise spectral correction method effectively improves the solutions, notable errors are still observed in some cases. It is therefore necessary to rigorously analyze the various sources of error for systematic and thorough improvement.

The work here identifies and quantifies the errors of PPMGCs that originates from various sources involving homogenization, condensation, spatial truncation, and low order transport approximation. A systematic analysis will be performed through numerical test calculations for PWR fuel assemblies and mini-core problems.

2. Error Sources of Pin-by-Pin Calculations

The standard flux-volume weighted MG-GCs are generated by the heterogeneous lattice transport calculations and the pin-level homogeneous calculations are carried out by lower order transport solvers. Therefore, among the four error sources detailed in Ref. [8], the spatial homogenization and the group-collapsing (condensation) effect are incorporated in the GCs while the transport and the spatial discretization errors are determined by the selection of the pin-by-pin solver.

2.1 Spatial Homogenization and Group Condensation

The spatial homogenization effect indicates not only the loss of heterogeneous cell geometry information but also the perturbation of GCs due to inconsistency of the cell boundary condition (B.C). In case of the assembly-wise two-step, for example, the lattice calculation to obtain the GCs commonly employs the zero current B.C. which is not valid in core environment. Consequently, the MG-GCs involve both the condensation and the homogenization errors.

The contributions of the two effects can be separated from the total as described in Ref. [9]. It starts from the following group condensation scheme:

$$\bar{\Sigma}_G^* = \left(\sum_{g\in G} \bar{\Sigma}_g^* \phi_g^* \right) \Big/ \left(\sum_{g\in G} \phi_g^* \right) = \sum_{g\in G} \bar{\Sigma}_g^* \tilde{\phi}_g^* \qquad (1)$$

where the asterisk, bar and tilde signs denote the reference core state, homogenization, and normalization of flux for the G–th group. The Core-GC and flux can be represented by the perturbation to the GCs and fluxes of all reflective single assembly (SA) results as:

$$\bar{\Sigma}_g^* = \bar{\Sigma}_g^{SA} + \Delta\bar{\Sigma}_g, \quad \phi_g^* = \phi_g^{SA} + \Delta\tilde{\phi}_g \qquad (2)$$

With these, the Core-GC is obtained as a sum of the SA-GC, the homogenization (E^{Hom}), condensation (E^{Con}) and the higher order error terms as in Eq. (3). The equation indicates that the MG-GCs obtained directly from a heterogeneous SA calculation would involve E^{Con} in the pin-homogenized calculation. For an assembly with the reflective B.C., for instance, the difference in neutron leakage prediction due to the homogenization changes the spectra which determines the E^{Con}.

$$\begin{aligned} \bar{\Sigma}_G^* &= \sum_{g\in G} \left(\bar{\Sigma}_g^{SA} + \Delta\bar{\Sigma}_g \right) \left(\tilde{\phi}_g^{SA} + \Delta\tilde{\phi}_g \right) \\ &= \sum_{g\in G} \begin{pmatrix} \bar{\Sigma}_g^{SA} \tilde{\phi}_g^{SA} \\ + \tilde{\phi}_g^{SA} \Delta\bar{\Sigma}_g + \bar{\Sigma}_g^{SA} \Delta\tilde{\phi}_g + \Delta\bar{\Sigma}_g \Delta\tilde{\phi}_g \end{pmatrix} \\ &= \bar{\Sigma}_G^{SA} + E_G^{Hom} + E_G^{Con} + O(E^2) \end{aligned} \qquad (3)$$

In the pin-by-pin calculation, the discontinuity factor (DF) or the SPH factor can correct both the homogenization and the condensation error simultaneously. Nevertheless, such equivalence factors (EFs) cannot consider E^{Hom} and additional changes in E^{Con} caused by adjacent assemblies because the standard EF generations are based on SA calculations.

2.2 Transport and Spatial Discretization

The pin-by-pin codes that solve the SPN equations with the FDM or a nodal method involve the transport and the spatial discretization effect. In the practical PPMGCs, the EFs also account for these effects. Accordingly, even the pin-by-pin diffusion FDM employing coarse mesh sizes, e.g. 1x1 or 2x2 meshes per pin, can yield good results by the aid of the EFs [3, 7]. Although it might be advantageous for practicality, the heavy dependence on the EFs is undesirable for the accuracy of solutions in general cases. It is clear that the EFs based on the SA can hardly incorporate the actual core environment.

3. Quantification of Each Error Source

The error sources presented in Section 2 correspond to each stage of the pin-level two-step core calculation. In this study, the magnitude of each error quantified step by step including the following four stages: 1) Method of Characteristics homogenized MG denoted by *MOC-47G* vs. *MOC-Het* comparison for isolating the pin-cell homogenization effect; 2) *MOC-XG* vs. *MOC-47G* for group-condensation, 3) *SPN-XG-32* vs. *MOC-XG* for low order transport approximation, and 4) *SPN-XG-M* vs. *SPN-XG-32* for spatial discretization.

MOC-Het denotes the 47G MOC calculation for the heterogeneous geometry while the *MOC-XG* is the *X* group MOC with homogenized pin-cells. The flat source MOC solver in nTRACER are used with the transport corrected P0 option and the ray parameters of a 0.01 cm ray spacing and 32 azimuthal and 4 polar angles per the octant sphere. Each pin was divided into 32x32 flat-source-regions for *MOC-XG* to eliminate the discretization effect. The *SPN-XG-M* denotes the *X* group diffusion (SP1) and SP3 FDM with *M*-by-*M* meshes per pin. All the cases do not use EFs.

The 2-, 4-, 8-and 47-GCs were obtained by the *MOC-Het* employing the group structure shown in Table I.

Table I: Structure of the condensed energy groups

Group	2G	4G	8G
Lower energy boundary (eV)			2.231E+6
			8.208E+5
		9.119E+3	9.119E+3
			1.301E+2
		3.928E+0	3.928E+0
	6.251E-1	6.251E-1	6.251E-1
			1.457E-1
	1.000E-4	1.000E-4	1.000E-4

The calculations were performed for 2-D assemblies and 3x3 CB type mini core problems. The assemblies have the 17x17 lattice structure. They are designated by fuel enrichment and the number of Pyrex burnable absorbers (BAs). The assembly specifications including the material and geometry are based on the VERA hot-zero-power core [11]. The assembly gap is, however, omitted for the simplicity. Configurations of the assemblies containing BAs are described in Fig. 1. The yellow, blue, cyan and red cells are fuel pins, guide tubes, instrument tubes and Pyrex BAs, respectively.

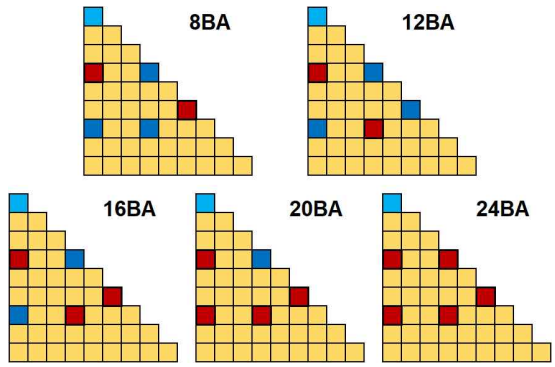

Fig. 1. Burnable absorber loading patterns of the assemblies

The mini core has the checkerboard arrangement consisting of five 2.11% 0BA and four 2.62% 24BA assemblies. To increase heterogeneity of the problem, the Ag-In-Cd (AIC) and the B_4C control rods are inserted in the central 2.11% 0BA assembly.

3.1 Analysis of 2-D Fuel Assemblies

The SPHINCS calculations are normally performed with 1x1 or 2x2 meshes per pin because the pin size is considered small enough to apply the finite difference approximation while finer mesh differencing requires demanding resources.

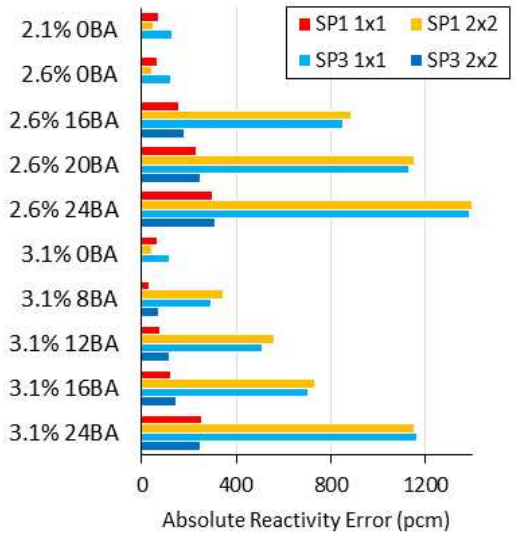

Fig. 2. Total reactivity error (pcm) of the pin-by-pin assembly calculations (*SPN-8G-M* vs. *MOC-Het*)

Fig. 2 shows the reactivity error of the SPHINCS pin-by-pin solutions for various problems quantified by comparing the *SPN-8G-M* solution with the corresponding *MOC-Het* solutions. These are the total errors in which all the components of errors are combined. Although SP3 calculations have less streaming effect than the diffusion and the mesh refinement decreases the FD error, *SP1-8G-1* agreed better than *SP3-8G-1* and *SP1-8G-2*. For the BA assemblies, the agreement of *SP1-8G-1* was even better than that of *SP3-8G-2*. It indicates there are significant error cancellations.

Tables II and III show the contribution of each error source to the apparent reactivity error of *SP1-8G-M* and *SP3-8G-M* for the 2.62% 24BA assembly. The homogenization (*Hom.*) and condensation (*Con.*) effect are omitted in Table III because those are considered independent of the SPN solver. Note that the same analyses with the 2-and 4-GCs were performed but the results are not presented since no notable difference was observed. In the case of the 2.62 24BA, for example, the condensation effect of 2G was only 67 pcm. The transport and the discretization effects were also slightly affected by the number of energy groups.

Table II: Significance of the error sources in the *SP1-8G-M* for the 2.619% 24BA assembly (Ref. k-inf: 0.925460)

Source	Specification	Err. (pcm)
Hom.	MOC-47G vs. MOC-Het	-708.0
Con.	MOC-8G vs. MOC-47G	34.8
Tran.	SP1-8G-32 vs. MOC-8G	-1529.6
Disc.	SP1-8G-1 vs. SP3-8G-32	2505.7
	SP1-8G-2 vs. SP3-8G-32	806.0
Sum of the sources of the **SP1-8G-1** (vs. total error)		302.9 (0.0)
Sum of the sources of the **SP1-8G-2** (vs. total error)		-1396.8 (0.0)

It is clearly shown in Table II that the agreement of *SP1-8G-1* is resulted from error cancellation. The diffusion case severely underestimates reactivity on the account of the transport effect (*Tran.*). More remarkable overestimation is, however, caused by the discretization effect (*Disc.*) cancelled out not only by the transport but also by the homogenization effect.

Table III: Significance of the error sources in the *SP3-8G-M* for the 2.619% 24BA assembly (Ref. k-inf: 0.925460)

Source	Specification	Err. (pcm)
Tran.	SP3-8G-32 vs. MOC-8G	-595.3
Disc.	SP3-8G-1 vs. SP3-8G-32	2654.7
	SP3-8G-2 vs. SP3-8G-32	956.8
Sum of the sources of the **SP3-8G-1** (vs. total error)		1386.2 (0.0)
Sum of the sources of the **SP3-8G-2** (vs. total error)		-311.8 (0.0)

In contrast, the result of *SP3-8G-2* was yielded by reduction of the transport and the discretization effect as shown in Table III. SP3 yielded about 900 pcm improvement of the transport error and the 2x2 mesh differencing per pin yielded about 1700 pcm decrease in the discretization error.

Although the details are not presented in the paper, the analysis can be applied for an arbitrary reaction rate and its result is consistent with the reactivity comparison. In case of the 2.619% 24BA assembly, for example, comparison of the source-normalized 1-group absorption rate for a corner pin-cell showed cancellation of the homogenization and the transport effect by the discretization effect. It yielded 0.73% error for the *MOC-47* vs. *MOC-Het* (*Hom.*), 0.14% for the *MOC-8G* vs. *MOC-47G* (*Con.*), 0.23% for the *SP3-8G-32* vs. *MOC-8G* (*Tran.*), -2.23% for the *SP3-8G-1* vs. *SP3-8G-32* (*Disc.*), and -1.14% for the *SP3-8G-1* vs. *MOC-Het*.

To observe the variation of the discretization error by the number of meshes per pin, test calculations were performed by decreasing the mesh size. Table IV shows the reactivity error of *SP3-8G-M* for 2.62% assemblies with the BA insertions. While the 0BA cases showed small discrepancies even with coarse meshes, the BA assemblies required at least 4x4 meshes to obtain the errors less than 500 pcm.

Table IV: Discretization error (pcm) of the *SP3-8G-M* for the 2.619% assemblies (vs. *SP3-8G-32*)

Mesh	1x1	2x2	4x4	8x8	16x16
0BA	-176.4	-55.0	-15.8	-4.1	-0.9
16BA	1628.9	594.1	177.7	45.5	9.2
20BA	2164.0	783.7	234.1	59.9	12.3
24BA	2654.7	956.8	285.7	73.2	15.1

3.2 Analysis of 3x3 Checkerboard Mini Cores

The objectives of the mini core calculations were to observe the reactivity error caused by the MG-GCs based on SA and to verify that the analysis can be applied for a larger problem which mimics a typical core center region. In addition to the GCs from SAs, the reference CB sets were generated by *MOC-REF*.

The contribution of each source to the total error is presented in Table V. Similar to the assembly cases, the SP3 agreed with MOC remarkably better than diffusion and the discretization error caused by the coarse mesh size was severe. Furthermore, the 2G vs. 8G comparisons provided some notable results that could not be observed from the SAs.

Con.(CB)s were obtained by *MOC-XG-CB* vs. *MOC-47G-CB* and correspond to the condensation error only, while *Con.(SA)s* were from *MOC-XG-SA* vs. *MOC-47G-CB* and are for the condensation error plus the neighbor effect. For the AIC rodded case, the group-condensing to 8G and 2G induces 70 and 397 pcm reactivity error. The neighbor effect brought about 17 and 132 pcm increases. The error reduction by the group

refinement was similar to the other cases. The results clearly show the need for MG-GCs in PPMGC.

On the other hand, the transport (*Tran.*) and discretization (*Disc.*) errors of 2G might be misleading. It seems as if the 2G calculation is more accurate than the 8G. However, the good agreement of 2G should be the result of error cancellation since the 2G is insufficient to incorporate the group dependent leakage effect [10]. The inaccurate surface current prediction is resulted from the insufficient resolution of energy ranges and it affects the pin-wise reaction rate distributions.

Table V: Significance of the error source in the *SP3-XG-M* for the 3x3 checkerboard mini core problems (unit: pcm)

CASE (Ref. k-eff)	1: N/A (1.007449)		2: AIC (0.980974)		3: B_4C (0.977874)	
Group	**8G**	2G	**8G**	2G	**8G**	2G
Hom.	**-198.5**		**-300.6**		**-308.0**	
Con. (CB)	**32.6**	136.8	**69.7**	396.9	**73.3**	442.5
Con. (SA)	**37.4**	195.1	**86.8**	528.7	**93.4**	594.9
Tran.	**-201.2**	-136.9	**-294.4**	-187.7	**-315.3**	-194.2
(Diffusion)	**(-497.8)**	(-378.0)	**(-717.5)**	(-491.5)	**(-756.3)**	(-497.3)
1x1, Disc.	**761.4**	612.6	**1046.1**	789.4	**1066.5**	772.3
Total	**399.1**	472.3	**538.0**	829.9	**536.6**	865.0
2x2, Disc.	**274.7**	218.7	**374.5**	280.8	**380.7**	274.5
Total	**-87.6**	78.3	**-133.7**	321.3	**-149.2**	367.2
4x4, Disc.	**81.9**	64.4	**111.7**	83.2	**113.5**	81.4
Total	**-280.5**	-76.0	**-396.5**	123.7	**-416.5**	174.0

4. Conclusions

The sources of the error in PPMGCs were identified quantitatively by analyzing their contribution to the total error. The calculations for SAs and 3x3 mini cores including the rodded configurations were carried out by the MOC, diffusion and SP3 FDM solvers with various energy groups and mesh discretization options.

The homogenization effect caused several hundred pcm error in the reactivity and the group condensation also yielded nontrivial errors for the problems with the significant heterogeneity such as the BA assemblies and the rodded mini cores. However, the two effects were considered less significant than the others because those can be captured successfully by the aid of EFs and the employment of MG-GCs. Therefore, the mitigation of the transport and the discretization effects would be a key measure to improve PPMGCs.

The transport effect was notable although SP3 yielded remarkable improvement of accuracy. For the mini core with B_4C control rod insertion, the transport error of the 8G SP3 was -315 pcm while the error of the 8G diffusion was -756 pcm. Thus, a higher order SPN such as the SP5 or a more rigorous approach like the method of discrete ordinates (SN) should be employed for further improvement.

Contrary to the general recognition that pin meshes are sufficiently small, this analysis showed that the coarse FD mesh causes severe errors and very fine mesh differencing is required to deal with the problems. For the B_4C rodded mini core, the error of the 8G SP3 was 1067 pcm with the 1x1 mesh per pin and 113 pcm with the 4x4 mesh. Considering excessive computing cost for fine-mesh whole core FDM calculation, it is strongly recommended to employ a nodal solver.

The presented results would provide the basis for further studies to develop more effective solvers employing various transport theories, including the SPN and the SN, and also nodal methods.

ACKNOWLEDGEMENT

This research is supported by the Brain Korea 21 Plus Program (No.21A20130012821).

REFERENCES

[1] M. Tatsumi and A. Yamamoto, Advanced PWR Core Calculation Based on Multi-group Nodal-transport Method in Three-dimensional Pin-by-Pin Geometry, J. of Nuc. Sci. Tech., Vol. 40, No. 6, pp. 376-387, 2003.
[2] U. Rohde et al., The reactor dynamics code DYN3D – models, validation and applications, Prog. Nucl. Energy, Vol. 89, pp. 170-190, 2016.
[3] J. I. Yoon, H. Hong, and H. H. Cho, Development of the High-Performance Pin-by-Pin Calculation Code with Planar Parallelization, Trans. Am. Nuc. Soc., Vol. 119, Orlando, Florida, November 11-15, 2018.
[4] A. Hebert, A Consistent Technique for the Pin-by-Pin Homogenization of a Pressurized Water Reactor Assembly, Nuc. Sci. Eng., Vol. 113, pp. 227-238, 1993.
[5] K. S. Smith, Assembly homogenization techniques for light water reactor analysis, Prog. Nucl. Energy, Vol. 17, pp. 303-335, 1986.
[6] H. H. Cho, H. Hong, H. G. Lee, and H. G. Joo, Preliminary Development of Simplified P3 based Pin-by-pin Core Simulator SPHINCS, Trans. of KNS Spring Meeting, Jeju, Korea, May 23-24, 2019.
[7] H. Hong and H. G. Joo, Leakage Feedback Method for Spectral Correction in Pin-Homogenized Multi-Group Core Calculations, Proc. of M&C 2019, Portland, Oregon, August 25-29, 2019.
[8] T. Kozlowski et al., Cell Homogenization Method for Pin-by-Pin Neutron Transport Calculations, Nuc. Sci. Eng., Vol. 169, pp. 1-18, 2011.
[9] Y. S. Ban and H. G. Joo, The Rationale of Leakage Parameters adopted in Leakage Feedback Method, Trans. of KNS Autumn Meeting, Yeosu, Korea, October 25-26, 2018.
[10] Y. S. Ban, Development of Advanced Leakage Feedback Method for Two-step Core Analyses, Ph.D. Thesis, Seoul National University, 2018.
[11] A. Godfrey, VERA Core Physics Benchmark Progression Problem Specifications, CASL-U-2012-0131-004, Oak Ridge National Laboratory, Consortium for Advanced Simulation of LWRs, Rev. 4, August 29, 2014.